Inositol 1,4,5-Trisphosphate-induced Calcium Release in the Organelle Layers of the Stratified, Intact Egg of *Xenopus laevis*

Jin-Kwan Han and Richard Nuccitelli

Department of Zoology, University of California, Davis, California 95616

Abstract. Using double-barreled, Ca^{2+}-sensitive microelectrodes, we have examined the characteristics of the Ca^{2+} release by inositol 1,4,5-trisphosphate (Ins(1,4,5)P$_3$) in the various layers of *Xenopus laevis* eggs in which the organelles had been stratified by centrifugation. Centrifugation of living eggs stratifies the organelles yet retains them in the normal cytoplasmic milieu. The local increase in intracellular free Ca^{2+} in each layer was directly measured under physiological conditions using theta-tubing, double-barreled, Ca^{2+}-sensitive microelectrodes in which one barrel was filled with the Ca^{2+} sensor and the other was filled with Ins(1,4,5)P$_3$ for microinjection. The two tips of these electrodes were very close to each other (3 μm apart) enabling us to measure the kinetics of both the highly localized intracellular Ca^{2+} release and its subsequent removal in response to Ins(1,4,5)P$_3$ injection. Upon Ins(1,4,5)P$_3$ injection, the ER-enriched layer exhibited the largest release of Ca^{2+} in a dosage-dependent manner, whereas the other layers, mitochondria, lipid, and yolk, released 10-fold less Ca^{2+} in a dosage-independent manner. The removal of released Ca^{2+} took place within ∼1 min. The sensitivity to Ins(1,4,5)P$_3$ and the time course of intracellular Ca^{2+} release in the unstratified (unactivated) egg is nearly identical to that observed in the ER layer of the stratified egg. Our data suggest that the ER is the major organelle of the Ins(1,4,5)P$_3$-sensitive Ca^{2+} store in the egg of *Xenopus laevis*.

A transient increase in intracellular free calcium concentration ([Ca^{2+}]$_i$) during sperm–egg interaction is one of the main ionic events of fertilization that triggers the initiation of development of the zygote (13, 21, 46, 60). This increase in [Ca^{2+}]$_i$ has been observed during the activation of a wide variety of eggs using at least three different techniques for Ca^{2+} measurement. The photoprotein, aequorin, was the first Ca^{2+} indicator to reveal a wave of increased free [Ca^{2+}]$_i$ after activation of the eggs of the medaka fish (16, 20, 39, 62), sea urchin (12, 48), starfish (10), frog (25), mouse (7, 8), and hamster (29). Pairs of Ca^{2+} electrodes were used to study the wave in frog eggs (3, 4, 35) and the fluorescent Ca^{2+} probe, fura-2, has been used in sea urchins (17, 51, 59).

Recent studies of sea urchin and frog eggs have indicated that sperm–egg interaction may release Ca^{2+} through the inositol lipid cascade. Sperm binding to its receptor at the egg surface activates a phosphoinositide-specific phospholipase C enzyme (24, 54, 55). The phospholipase C enzyme hydrolyzes phosphoinositol 4,5-bisphosphate (PIP$_2$)[1] producing two second messengers, inositol 1,4,5-trisphosphate (Ins(1,4,5)P$_3$) and diacylglycerol. Ins(1,4,5)P$_3$ releases Ca^{2+} from intracellular Ca^{2+} stores whereas diacylglycerol activates the phospholipid- and Ca^{2+}-dependent protein kinase, protein kinase C, which is involved in many cellular re-

sponses such as cell alkalinization (43, 47). This hypothesis that the PIP$_2$ pathway is involved in animal egg activation has been partially tested in at least three phyla, sea urchin (43, 47, 54, 55), frog (24), and hamster (28).

The fertilized egg of the frog, *Xenopus laevis*, exhibits a transient increase in intracellular Ca^{2+} from 0.4 to 1.2 μM beginning within the first 2 min after fertilization, and returning to its original value by the end of 10 min (3). It has also been observed that the microinjection of sufficient Ins(1,4,5)P$_3$ into the *Xenopus* egg can trigger a Ca^{2+} release from intracellular stores (4) that is indistinguishable from that observed at fertilization (3). In this study, we have attempted to identify the Ins(1,4,5)P$_3$-sensitive Ca^{2+} storage site(s) in eggs of *Xenopus laevis*. Organelles and other cellular components of the *Xenopus* egg can be easily stratified into separate layers by centrifugation within an intact living cell. This allows us to perform our experiment in the relatively physiological conditions of intact egg cytoplasm rather than as an organelle fraction prepared by homogenation and purification which exposes the cell components to unphysiological conditions. Stratified eggs exhibit unique organelle layers: lipid-, ER-, mitochondria-, pigment-, and yolk-enriched layers that partitioned within the cytoplasm based on their density. The organelles in each layer were identified by EM. The intracellular Ca^{2+} concentration in each layer was directly measured using Ca^{2+}-sensitive microelectrodes. We used a novel theta-tubing, double-barreled Ca^{2+}

1. *Abbreviations used in this paper:* CG, cortical granules; Ins(1,4,5)P$_3$, inositol 1,4,5-trisphosphate; pCa, negative log of free calcium; PIP$_2$, phosphoinositol 4,5-bisphosphate.

electrode in which one barrel was used as the Ca^{2+} sensor and the other for $Ins(1,4,5)P_3$ microinjection based on the design of Munoz et al. (32). The advantage of this technique over previous ones is that the two tips of the theta-tubing electrode are very close to each other (~3 μm apart) so we were able to measure the $[Ca^{2+}]_i$ close to the $Ins(1,4,5)P_3$ injection site.

In this study we report the direct measurements of the local intracellular free Ca^{2+} release in response to $Ins(1,4,5)P_3$ microinjection in the organelle-stratified, centrifuged *Xenopus* egg. The ER-enriched layer releases the largest amount of Ca^{2+} whereas other layers release much smaller amounts. The amount of Ca^{2+} released from the ER is dose dependent, and this Ca^{2+} is removed within 1 min after release.

Materials and Methods

Centrifugation of Eggs

Xenopus eggs were obtained by squeezing females that had been induced to ovulate via injection of 800 IU of human chorionic gonadotropin (Sigma Chemical Co., St. Louis, MO) 8–10 h earlier. The eggs were dejellied by gentle agitation in 2% L-Cystein in F1 solution (31.25 mM NaCl, 1.75 mM KCl, 0.5 mM Na_2HPO_4, 1.0 mM $CaCl_2$, 0.06 mM $MgCl_2$) with pH adjusted to 7.8 with NaOH. After washing extensively with F1, eggs were suspended at the interface formed between 5 ml of 30% Ficoll solution and 5 ml of F1 solution (similar procedures in *Rana pipiens* oocytes had been described in reference 27). 10 mM chlorobutanol was added to the F1 solution to reduce the likelihood of activation during centrifugation. Centrifugation was conducted in a centrifuge (RC-5B; Sorvall Instruments, Newton, CT) with HB-4 rotor at 4,080 g for 1 h at 18°C. The stratified eggs were removed from the F1/Ficoll cushion interface and transferred to the small plexiglass chamber filled with 30% Ficoll-F1 (without chlorobutanol) for these studies.

Construction of the Double-barreled, Ca^{2+}-specific Microelectrodes

Electrode construction combined the methods of Busa's modified version (3), Tsien and Rink (52, 53), and Munoz et al. (32). In brief, chromic acid-cleaned, borosilicate glass, theta-tubing capillaries were pulled to form submicrometer tips with a shoulder-tip length of 1.0 cm, beveled at a 45° angle to an open width of ~5.0 μm across the bevel. The Ca^{2+} electrode barrel was silanized with aminosilane as described by Munoz et al. (32). The silanized barrel was then back filled with pCa 7.0 (negative log of free Ca^{2+} concentration) calibration buffer and the tip was filled via suction with a 100–150-μm-long column of unjelled Ca^{2+} sensor, (ETH 1001; Fluka Chemical, Ronkonkoma, NY) while blowing air into the other barrel (to be used for $Ins(1,4,5)P_3$ injection) to prevent filling both with Ca^{2+} sensor. The electrode tips were then briefly dipped twice into polyvinyl chloride-gelled Ca^{2+} sensor and dried in the air for 15 min after each dip. The microelectrodes were first conditioned by immersing their tips for 0.5–3 h in the pCa 7.0 buffer solution before calibration and adopted when their response ranged from 26–29 mV per 10-fold change in $[Ca^{2+}]_i$. On average, about one out of three electrodes met this criterion without giving detectable electrical drifting. Injection barrels were back filled with 2 μl of the microinjection solution just before cell impalement.

Membrane potential microelectrodes with submicrometer tips were pulled from borosilicate glass tubing that contained an inner fiber, and were backfilled with 0.5 M KCl, 10 mM EGTA (pH 7.4). Their resistance ranged from 7 to 15 MΩ in F1.

Electrophysiological Recordings and Microinjection

Experiments were performed in a 3-mm-deep plexiglass chamber with a glass coverslip bottom. The bath was grounded via an Ag/AgCl wire in an F1-agar-filled tube. The membrane potential electrode was connected to a standard electrophysiological amplifier (AM-4; General Bio-engineering, Valley Center, CA). The calcium electrode was connected to a unity-gain, high-input impedance amplifier (311J; Analog Devices, Inc., Northwood, MA). Subtraction of membrane potential from the Ca^{2+} electrode output

was performed by using a differential input on the chart recorder and the oscilloscope.

Calcium microelectrodes were calibrated in buffers of pCa 6.0, 6.5, 7.0. These contained 10 mM EGTA, 5 mM $CaCl_2$; (for pCa6.0) 10 mM Pipes, 45 mM KOH, 15 mM KCl (pH 6.77 at 23°C); (for pCa 6.5) 10 mM Pipes, 47 mM KOH, 12 mM KCl (pH 7.02 at 23°C); and (for pCa 7.0) 10 mM 4-MOPS, 35.5 mM KOH, 29.3 mM KCl, pH 7.27, at 23°C). These buffers' ionic strength was 150 mOsm, close to that of *Xenopus* egg cytoplasm (34, 58). We used the "mixed constants" for EGTA to calculate the resulting free Ca^{2+} levels after correction for ionic strength as discussed on page 45 of reference 50. It usually took a few seconds to change buffers completely (~10 times the original volume). Although it is difficult to estimate the exact response time of the Ca^{2+}-specific electrodes, the average response time from pCa 7.0 to pCa 6.5 was 2.2 s (SD = 0.7, n = 9) and from pCa 6.5 to pCa 6.0 was 1.9 s (SD = 0.9, n = 9). Those numbers were calculated using as a start time the point at which the chart recorder pen began to move fastest during the solution change. The maximum pen response time measured was 0.3 s to traverse 25 cm. In response to $Ins(1,4,5)P_3$ injections the average electrode response time was 0.5 s (SD = 0.07, n = 32).

The most aggravating problem faced by those using Ca^{2+} microelectrodes is the electrodes' fairly frequent failure to calibrate identically before and after cell impalement. Calibration curves may either be displaced by many mV after withdrawal from the cell, or the electrode response may be reduced, or both. One way to minimize this baseline shift is to impale a cell a few times with a newly constructed electrode before beginning an experiment. If the electrode still calibrates well, it is less likely to shift its output baseline with subsequent impalements. Throughout the experiments, electrodes were calibrated before and after cell impalement; only data from those displaying nearly identical recalibrations (within 3 mV) after impalement were used for the quantification of intracellular Ca^{2+} concentration. Another major technical problem with Ca^{2+} microelectrodes is a reduced sensitivity to Ca^{2+} at the final calibration after impalement. This was most common after rather long experiments of 3 h or so. In such cases, of course, the data were discarded. Such difficulties resulted in few reliable data sets compared with the number of attempts that have been made (4 out of 15 in the iontophoresis experiment, and 5 out of 22 in the pressure injection experiment).

Microinjections were performed either iontophoretically or by pressure. For iontophoresis, injection barrels were loaded with 1-mM solutions of either $Ins(1,4,5)P_3$, inositol-1,4-bisphosphate, or fructose-1,6-bisphosphate as specified, in every case in 0.1 mM Hepes, pH 7.8. All chemicals were purchased from Sigma Chemical Co. Electrical connection with this filling solution was made via an Ag/AgCl wire glued into the injection barrel. Negative current was injected using the constant current injection circuit of a preamplifier (model AM-4; General Bio-engineering), and current commands were supplied to the amplifier through a stimulus isolator (model 305; W-P Instruments, Inc., New Haven, CT) by an Anapulse stimulator (model 301; W-P Instruments Inc.). The injected current was monitored at the current monitor output of the amplifier using an oscilloscope with a digital waveform analyzer (model 5D10; Tektronix, Inc., Beaverton, OR), and both this oscilloscope and a chart recorder were used to record the Ca^{2+} electrode output. The electrical artifact generated at the Ca^{2+} electrode by the iontophoretic current injection was corrected by subtracting the amplitude of the recording obtained by the injection of $Ins(1,4,5)P_3$ into the calibration buffer outside of the egg from the electrode's response to $Ins(1,4,5)P_3$ injection in the egg.

For pressure injections, one of the barrels of the double-barreled electrode was loaded with injection solution and connected to a picospritzer (General Valve, Fairfield, NJ). Pressures ranging from 20 to 30 psi for 0.1–5 s were used for the injections. The volume with these pressure ranges were measured by injecting into oil before and after experiments. Volumes injected varied from 4.2×10^{-15} to 6.3×10^{-12} liters. However, the exact volume injected in each experiment was difficult to estimate since the pre- and post-calibration was usually not the same. This inconsistency was due to the clogging of the injection barrel with a sticky egg cytoplasm during the experiments.

EM

Centrifuged eggs were fixed in 3% glutaraldehyde in F1 for 3 h, washed with F1 four times, and then postfixed in 1% osmium tetraoxide for 1 h. After washing with F1 two times, eggs were dehydrated with an acetone series, embedded in plastic, and sectioned. Sections were poststained with uranyl acetate in 70% ethanol for 5 min and examined with an electron microscope (model 410; Philips Electronic Instruments, Inc., Mahwah, NJ).
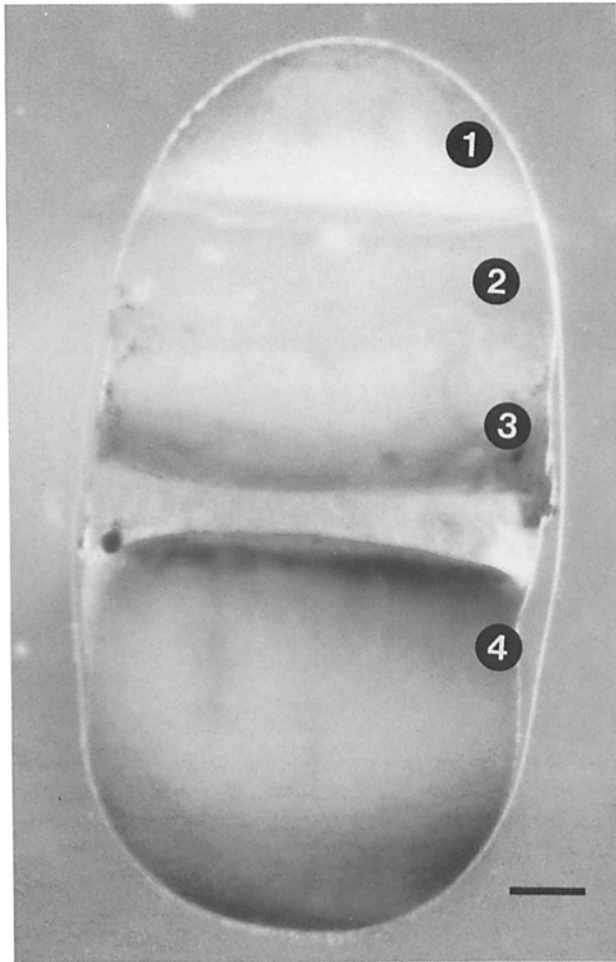
Figure 1. Photomicrograph of a stratified *Xenopus laevis* egg after centrifugation in F1 on a 30% Ficoll layer at 4,080 *g* for 1 h. Four organelle-enriched layers are indicated: (*1*) lipid layer; (*2*) ER layer; (*3*) mitochondria layer; and (*4*) yolk layer. Bar, 0.2 mm.

Results

Previous experiments demonstrated that microinjection of Ins(1,4,5)P₃ into *Xenopus laevis* eggs released Ca²⁺ from intracellular stores, and for sufficiently large doses the characteristic wave of intracellular Ca²⁺ release induced by Ins-(1,4,5)P₃ was indistinguishable from that observed during fertilization (4). In these experiments we tried to identify the Ins(1,4,5)P₃-sensitive Ca²⁺ storage organelle in frog eggs by stratifying the organelles by centrifugation and using double-barreled Ca²⁺ microelectrodes. Fig. 1 shows a light micrograph of an organelle-stratified *Xenopus* egg consisting of morphologically distinct layers in the order of their specific densities. EM indicates that the top milky layer is composed largely of lipid droplets, the transparent layer is composed mainly of smooth and rough ER microsomes (5), the opaque layer is mainly composed of mitochondria, and the bottom yellow layer is composed of yolk platelets with a thin layer of pigment on top (Fig. 2). There is very little contamination of other organelles in the ER microsome layer, but some microsomes can be seen in the lipid, mitochondria, and yolk layers. A small number of mitochondria could also be found in the yolk layer. We also observed cortical granules (CG)

along the cortex of the stratified eggs, suggesting that they were probably unactivated (Fig. 3). We have examined the characteristics of Ca²⁺ release in the four major layers (lipid, ER, mitochondria, yolk) of centrifuged eggs using double-barreled, Ca²⁺-specific microelectrodes made from theta-tubing. Microelectrodes incorporating a Ca²⁺-selective tip adjacent to an Ins(1,4,5)P₃ injection barrel (<3 μm away) were introduced into each layer ∼30–80 μm below the plasma membrane, and the microinjection of Ins(1,4,5)P₃ was accomplished either by iontophoresis or by pressure.

Ca²⁺ Release Characteristics of the ER Layer

We have repeated the iontophoresis experiments 15 times. In 7 of the 15 iontophoresis experiments the Ca²⁺ electrode lost sensitivity during the experiment and in 4 cases it showed a large electrical shift or a nonlinear Nernstian response upon recalibration (we only accepted data from electrodes that exhibited a response of 26–29 mV per 10-fold [Ca²⁺]ᵢ change). This left four reliable measurements. Iontophoresis of Ins(1,4,5)P₃ into the ER-enriched layer releases Ca²⁺ in ∼0.5 ± 0.07 s (*n* = 32) and the injection of increasing amounts of Ins(1,4,5)P₃ demonstrated a near linear dose-response relationship (Fig. 4 and Fig. 5). In two of the four iontophoresis experiments, the amplitude of the increase in [Ca²⁺]ᵢ was linearly proportional to log of the Ins-(1,4,5)P₃ injected (Fig. 5, *C* and *D*). In two other cases, the increased [Ca²⁺]ᵢ was linearly proportional to the amount of Ins(1,4,5)P₃ injected (Fig. 5, *A* and *B*).

The minimum amount of Ins(1,4,5)P₃ required to generate a detectable Ca²⁺ release in one particular recording (Fig. 4) was ∼0.027 nC of iontophoretic charge. However, this number varied from 0.02 to 0.2 nC among recordings due to slight differences in both electrodes (it is difficult to construct double-barreled electrodes with identical response characteristics) and the local density of Ins(1,4,5)P₃-sensitive organelles. The amount of Ins(1,4,5)P₃ delivered from the 0.02 nC of injection current can be estimated by the formula $q = nI/zF$, where q is the amount of charge in moles, n is the transport number, I is the amount of charge injected, z is the charge number of the ion, and F is Faraday's constant (37). If one assumes that half of this current is carried by Ins(1,4,5)P₃ with a net charge of −4, this much current would generate a local maximum concentration of 100 nM within a spherical region 40 μm in radius. This radius was calculated from the diffusion equation in three dimensions as the distance Ins(1,4,5)P₃ would diffuse within 0.5 s using a diffusion constant of 6 × 10⁻⁶ cm²s⁻¹ (measured for glucose in dilute aqueous solution). This diffusion distance is surely an upper limit since the Ins(1,4,5)P₃ diffusion constant in egg cytoplasm is likely to be smaller than that of glucose in dilute aqueous solution due to the slightly larger molecular weight and the enhanced viscosity of the organelle-rich cytoplasm. In most eukaryotic cells the viscosity of cytoplasm has been found to be two to six times higher than that of water; and FRAP studies in living cells indicated that even the smallest intracellular proteins diffuse at least three times more slowly in cytoplasm than in dilute aqueous solution, regardless of charge or binding specificity (see reference 26 for review).

Besides using iontophoretic delivery of the Ins(1,4,5)P₃ into the stratified egg, we also have injected the Ins(1,4,5)P₃ by pressure. The pressure injection method had the addi-
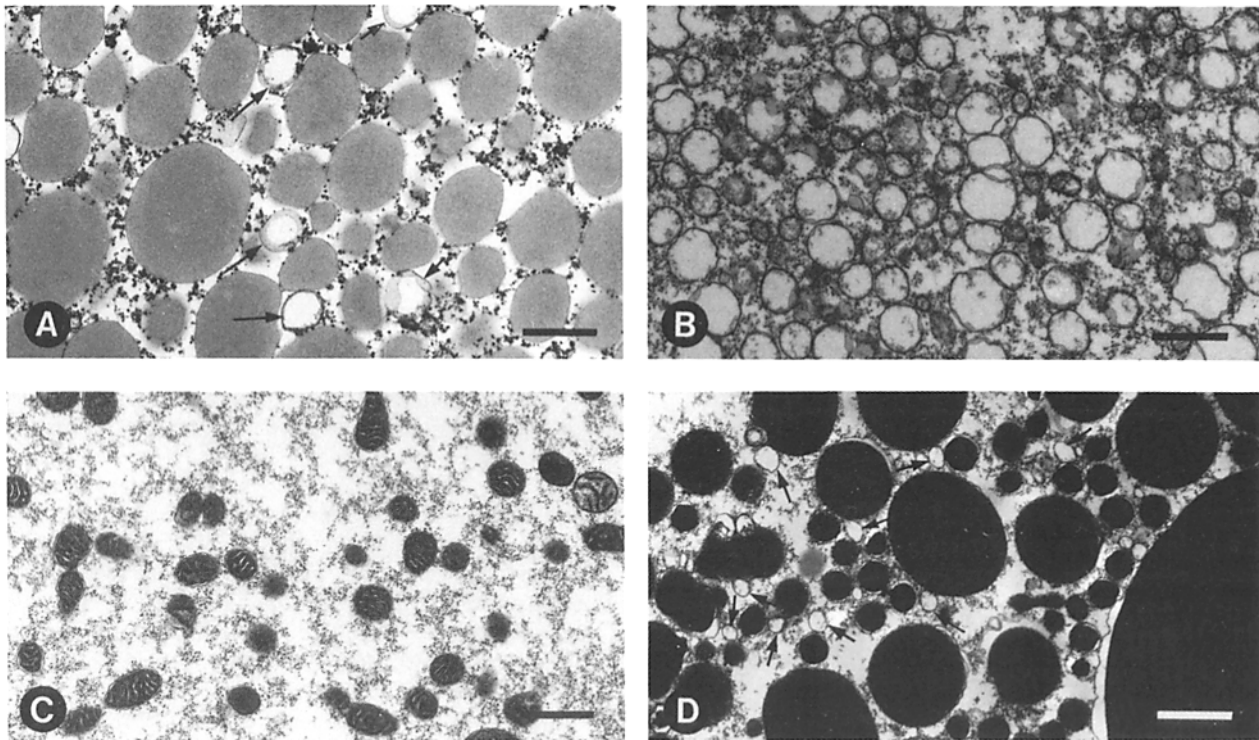
Figure 2. Electron micrographs of the four major stratified layers. (*A*) lipid; (*B*) ER; (*C*) mitochondria; (*D*) yolk. Some microsomes (indicated by *arrows*) are seen in the lipid and yolk layers. Bars: (*A–C*) 1 μm; (*D*) 3 μm.

tional problems of injected barrel clogging and, in some cases, vibration of the electrode upon pressure pulse application. Electrode vibration usually resulted in a large, intracellular Ca^{2+} increase near the electrode regardless of which organelle layer was being investigated. It is likely that this increase was due to the movement of extracellular Ca^{2+} into the cell when the electrode-membrane seal was damaged since such increases were not observed when the electrode did not vibrate. Nevertheless, we have five reliable experiments using pressure injection that are summarized in Fig. 6. The estimated amount of Ins(1,4,5)P$_3$ injected by pressure ranged from 16 nM to 23 μM in the sphere with a 40-μm radius centered around the injection barrel. As a control we have iontophoresed 32 nC of both 1.0 mM of fructose 1,6-bisphosphate and 1.0 mM of Ins(1,4)P$_2$. Neither of these injections stimulated Ca^{2+} release from the ER-enriched layer.

The [Ca^{2+}]$_i$ in the ER-enriched layer returned to within 5% of its original level within 47.4 $\pm$ 5.1 s ($n = 5$) after the peak release of intracellular Ca^{2+} (765 $\pm$ 32 nM, $n = 5$) induced by Ins(1,4,5)P$_3$ injection (Fig. 7). The kinetics of Ca^{2+} uptake into the ER-enriched layer after injection of Ins(1,4,5)P$_3$ were composed of a rapid phase at the beginning and slower phase at the end. Approximately 73 $\pm$ 8.2% ($n = 5$) of the released Ca^{2+} was removed within the first 10 s and the remaining Ca^{2+} was taken up in the next 60 s. We have tried to compare the characteristics of Ca^{2+} uptake in the ER layer with other layers, however, the amount of Ca^{2+} release induced by Ins(1,4,5)P$_3$ from the non-ER layers was too small for the uptake to be analyzed reliably.

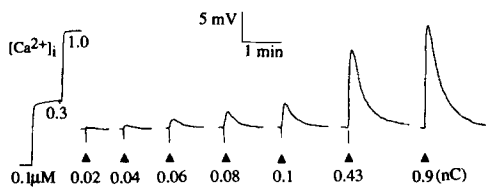## Ca^{2+} Release Characteristics of the Other Organelle Layers

In contrast to the large release of Ca^{2+} in the ER microsome layer, microinjection of Ins(1,4,5)P$_3$ into each of the other layers released little intracellular Ca^{2+} (Fig. 8). Fig. 9 shows the relative Ca^{2+} release in each of four layers as a function of the amount of Ins(1,4,5)P$_3$ iontophoresis current. In a typical ER layer the [Ca^{2+}]$_i$ increases to 780 nM in response to 0.9 nC of Ins(1,4,5)P$_3$ injection current (43 μM of Ins(1,4,5)P$_3$ in the sphere with a 40-μm radius centered around the injection barrel), whereas in other layers the [Ca^{2+}]$_i$ increases by <80 nM in response to the same Ins(1,4,5)P$_3$ dose and does not exhibit dosage dependence. The small release of Ca^{2+} from the non-ER layers might be due to a small contamination of ER microsomes in these layers since the electron micrographs show some microsomal vesicles in the layers of mitochondria, lipid, and yolk. The characteristics of the increase in [Ca^{2+}]$_i$ by Ins(1,4,5)P$_3$ injection in the unstratified (unactivated) egg is almost identical to that of the ER layer in the stratified egg (Fig. 9).

As previously mentioned, both the variability in electrode response characteristics and the variable organelle density at the site of impalement resulted in a wide range of Ca^{2+} release to a given Ins(1,4,5)P$_3$ dose. This led us to normalize the data so that these results could be pooled. A range of Ins(1,4,5)P$_3$ injections was carried out in each layer of several stratified eggs and the dose of Ins(1,4,5)P$_3$ eliciting a maximal response from the ER layer was determined. The
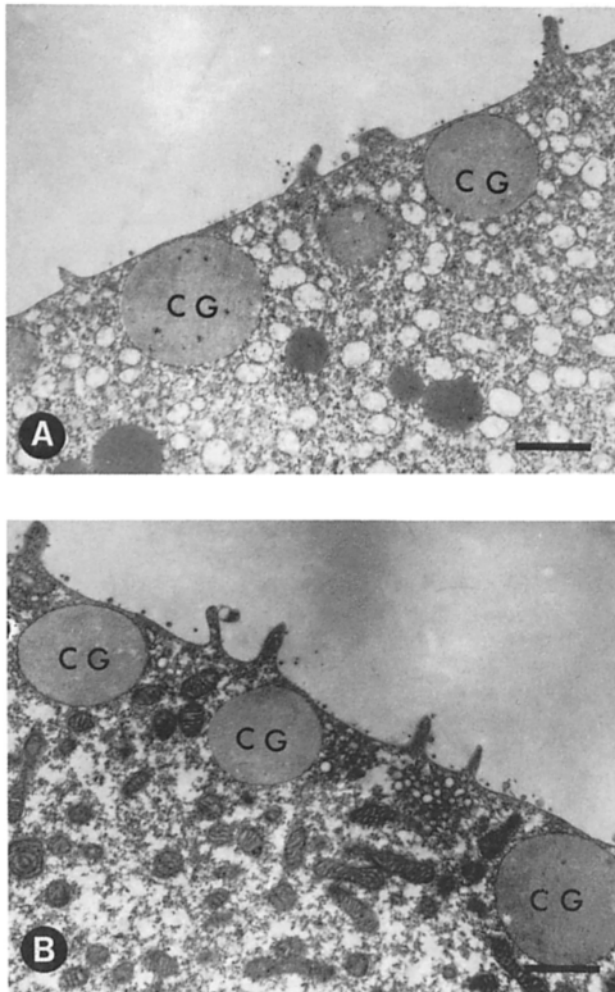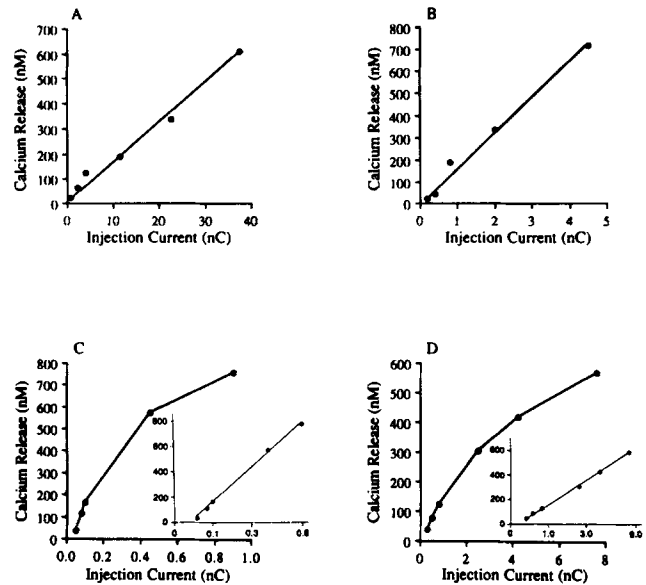
Figure 3. High magnification electron micrographs of the cortex of a stratified egg. Intact *CGs* are seen along the cortex of the ER-enriched microsome layer (*A*), and of the mitochondria-enriched layer (*B*). Bars, 1 μm.

Figure 5. Dose-response curves of Ins(1,4,5)P$_3$-induced release of Ca^{2+} from ER-enriched layer. The amount of Ca^{2+} release from this layer is a either linearly (*A* and *B*) or log-linearly (*C* and *D*) proportional to the Ins(1,4,5)P$_3$ injection. *Inset,* the same data (*C* and *D*) were plotted in the semilogarithmic paper. The amplitude of the intracellular Ca^{2+} release is linearly proportional to the log of the Ins(1,4,5)P$_3$ injected.

Discussion

New Findings

We had previously found that the injection of Ins(1,4,5)P$_3$ into the intact *Xenopus* egg transiently releases an amount response of the other organelle layers to this same dose was then determined and is summarized in Fig. 9. Although the amount of Ins(1,4,5)P$_3$ needed to elicit a given intracellular Ca^{2+} increase in each layer differed from experiment to experiment, it was generally 10-fold less effective in releasing Ca^{2+} in non-ER layers than in the ER-enriched layer.

Figure 4. Tracing of intracellular Ca^{2+} recordings during iontophoresis with Ins(1,4,5)P$_3$ into the ER-enriched layer. Trace at left in this figure shows Ca^{2+}-electrode calibrations (0.1, 0.3, 1.0 μM) before impalement. The resting level of Ca^{2+} concentration in the ER layer is ∼0.25 μM. The depth of the Ca^{2+} electrode in this layer was between 30–80 μm. We found that the depth of the electrode in the stratified egg did not affect the measurement of the Ca^{2+} release. The threshold for Ca^{2+} release in this particular recording is ∼0.027 nC of iontophoretic charge.

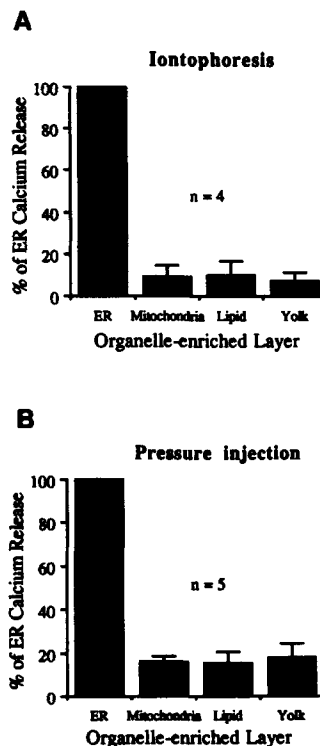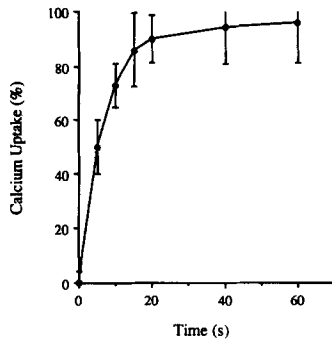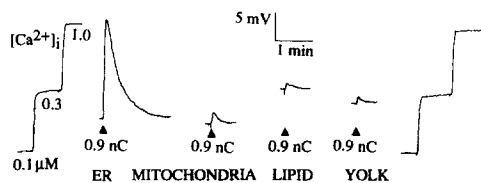*Figure 6.* Comparison of the Ins(1,4,5)P$_3$ response in four major layers of the stratified egg. All data from the iontophoresis (*A*) and the pressure injection (*B*) experiments are normalized. For a given amount of the Ins(1,4,5)P$_3$ injection, the mitochondria, lipid, and yolk layers released less than one-tenth of the Ca^{2+} released by the ER layer.
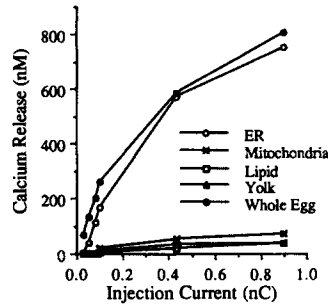
Figure 7. Calcium uptake in the ER-enriched layer. Recovery time for the released Ca^{2+} was measured from the peak of the Ca^{2+} increase induced by a given amount of $Ins(1,4,5)P_3$ injection to the time at which the $[Ca^{2+}]_i$ level had returned to within 5% of the preinjection value. Data points are the mean $\pm$ SD of five separate determinations.

Figure 9. Increases in $[Ca^{2+}]_i$ in each of four layers in a stratified Xenopus egg as a function of the amount of $Ins(1,4,5)P_3$ iontophoresis current passed through the other barrel of a double-barreled, Ca^{2+}-specific microelectrode. For comparison, the response measured in an unstratified egg is included. In the ER layer, $[Ca^{2+}]_i$ increased to ~770 nM in response to 0.9 nC of iontophoretic current. The same amount of the injection current, resulted in a 74-nM $[Ca^{2+}]_i$ increase in mitochondria-enriched layer and a 37-nM $[Ca^{2+}]_i$ increase in both lipid- and yolk-enriched layers. The $[Ca^{2+}]_i$ increase in an unstratified egg was similar to that of the stratified ER layer.

of cytoplasmic free Ca^{2+} locally from intracellular stores that is proportional to the amount of $Ins(1,4,5)P_3$ injected (3). If a threshold Ca^{2+} level is reached, it triggers a wave of increased free Ca^{2+} that spreads over the egg and initiates the early events of egg activation such as the membrane depolarization, cortical contraction, and CG exocytosis. In this report, we have directly demonstrated that the ER-enriched layer of the stratified egg exhibits a 10-fold larger Ca^{2+} release upon $Ins(1,4,5)P_3$ injection than the other organelle-enriched layers. This was accomplished by combining two novel techniques, the Ca^{2+}-sensitive double-barreled microelectrode technique, and organelle stratification by centrifugation of intact eggs. Both techniques are crucial for this study. Among the various methods for measuring intracellular free Ca^{2+}, the Ca^{2+}-specific microelectrode has the best spatial resolution and provides the most accurate absolute Ca^{2+} level. Using the double-barreled electrode we can accurately measure the local $[Ca^{2+}]_i$ a few micrometers from the site of $Ins(1,4,5)P_3$ injection. Centrifugation of living eggs stratifies the organelles yet retains them in a more physiological condition than other methods such as cell fractionation or permeabilization which would disturb the cell membranes and the normal cellular environment. We have found that for a given amount of $Ins(1,4,5)P_3$, the ER-enriched layer releases ~10-fold more Ca^{2+} than the other

organelle layers. The amount of intracellular Ca^{2+} increase in the ER layer in response to $Ins(1,4,5)P_3$ injection was dose dependent. This dose dependency was unique to the ER layer since no other organelle layer showed a dose-dependent response.

Comparison to Previous Studies of Ca^{2+} Release

Most previous studies of $Ins(1,4,5)P_3$-induced Ca^{2+} release have utilized either cell-free systems or permeabilized cells. In general, these studies have shown that the intracellular Ca^{2+} release is linearly proportional to the concentration of $Ins(1,4,5)P_3$ for low doses and it plateaus for higher doses where most of the Ca^{2+} pools were depleted by $Ins(1,4,5)P_3$ (6, 9, 19, 22, 23, 30, 33, 38, 41, 45, 56, 61). We have observed both linear and log-linear responses that do not appear to be correlated with the amount of $Ins(1,4,5)P_3$ injected. These different responses may depend on the proximity of the $Ins(1,4,5)P_3$-sensitive Ca^{2+} store in each case. At the present time we are unable to determine which of the two responses is more physiological.

We know of only two previous studies using intact cells that obtained similar information. Payne and Fein (36) showed that $Ins(1,4,5)P_3$-induced Ca^{2+} release was localized to the R-lobe of the Limulus photoreceptor where prominent cisternae of smooth ER are uniquely localized within this cell. They concluded that these cisternae are the probable site of $Ins(1,4,5)P_3$ action. Eisen and Reynolds (11) stratified sea urchin eggs by centrifugation and studied the wave of Ca^{2+} release following fertilization. They observed that the "clear zone" which was enriched in ER in these stratified eggs was the source of Ca^{2+} release as indicated by aequorin luminescence.

A third approach that has yielded specific information regarding $Ins(1,4,5)P_3$ receptor distribution follows the recent isolation of the $Ins(1,4,5)P_3$ receptor from the mouse cerebellum (14, 15, 40, 44). Antibodies generated to this protein have been used in immunocytochemical studies to demonstrate that the $Ins(1,4,5)P_3$ receptor is found on the ER in these cells. Unfortunately, these antibodies do not cross react with Xenopus so we have been unable to apply that technique in this system.

Figure 8. Tracings of double-barreled Ca^{2+}-specific microelectrode recordings during iontophoresis with the same amount of $Ins(1,4, 5)P_3$ (0.9 nC) into different layers of a stratified egg. Trace at left and right in this figure shows Ca^{2+}-electrode calibrations (0.1, 0.3, 1.0 μM) before and after impalement. Each layer exhibited a slightly different level of resting $[Ca^{2+}]_i$ concentration. When the same amount of $Ins(1,4,5)P_3$ iontophoretic current was injected, the ER-enriched layer released the most Ca^{2+} whereas the other layers released little. One possibility is that the small release of Ca^{2+} from non-ER layers is due to the small contamination of ER microsomes in these layers. In all tracings in this figure, the electrical artifact due to the iontophoretic current injection (a brief, 2–3 mV blip) was corrected for by subtracting from the $Ins(1,4,5)P_3$-induced response an amount equal to the amplitude of the small change resulting from the response recorded when $Ins(1,4,5)P_3$ was injected into the pCa 7.0 calibration buffer outside of the egg.

Ca²⁺ Uptake Kinetics

The Ca²⁺ released by Ins(1,4,5)P₃ was removed quickly in the ER-enriched layer. The Ca²⁺ uptake kinetics in the ER-enriched layer were composed of two phases, the initial rapid phase followed by the slower phase which agrees with observations on ATP-dependent Ca²⁺ uptake characteristics from many cell types (22, 23, 31, 42, 56, 61). However, we have found that the rate of the Ca²⁺ removal was far faster than that found in other studies. In the ER-enriched layer ∼95% of the locally released Ca²⁺ was removed within 47.4 ± 5.1 s (n = 5), as compared with previous biochemical measurements in other systems with uptake times ranging from several to tens of minutes. Up to now, most kinetic studies of Ca²⁺ release and uptake have been done by measuring ⁴⁵Ca²⁺ flux in either permeabilized cells or ER microsome fractions. Under these circumstances, it is difficult to determine the kinetics of Ca²⁺ flux reliably, due to uncertainties in diffusion times and the difficulty of aliquot acquisition at very short intervals. In this respect the techniques introduced here are more reliable indicators of the kinetics of Ca²⁺ movement.

Ca²⁺-release Response of Non-ER Layers

The small response of the non-ER layers to Ins(1,4,5)P₃ may well be due to the small contamination of ER microsomes in those layers. Another possibility is that an unidentified, Ins(1,4,5)P₃-sensitive Ca²⁺ store exists that is not separable under the rather mild centrifugal force (4,080 g) performed in this experiment. One candidate is the recently discovered cytoplasmic organelle called the "calciosome" (18, 57) which is Ins(1,4,5)P₃ sensitive. Calciosomes have been identified as discrete organelles (much smaller than the ER) distributed throughout the cytoplasm and characterized by a calsequestrin-like protein in nonmuscle cells. Further work with a calciosome marker such as an antibody to calsequestrin should determine if this organelle is present in the stratified egg. However, even if it is present, the 10-fold higher Ins(1,4,5)P₃ sensitivity of the ER-enriched layer indicates that an organelle which can be stratified by centrifugation is more likely to be the main target for Ins(1,4,5)P₃ in this cell. Furthermore, the Ins(1,4,5)P₃ sensitivity of the stratified ER layer is quite comparable to that of the cortex of an unstratified, unactivated egg. This also suggests that the ER-enriched layer contains the main Ca²⁺-releasing organelle, and that the concentration of this organelle in the cortex is comparable to its concentration in the stratified layer.

Previous work (3) demonstrated that the *Xenopus* egg possesses at least two functionally distinct intracellular Ca²⁺ pools: an Ins(1,4,5)P₃-sensitive pool and an Ins(1,4,5)P₃-insensitive (ionophore, A23187-sensitive) pool. Although we have directly demonstrated that the ER is an Ins(1,4,5)P₃-sensitive Ca²⁺ pool, we have not attempted to identify the Ins(1,4,5)P₃-insensitive Ca²⁺ pool that is believed to be involved in Ca²⁺ release deep in the cell. Studies using permeabilized hepatocytes (49) and clonal pituitary (GH3) cells (1) suggest the possibility that the Ins(1,4,5)P₃-insensitive Ca²⁺ store is a subgroup of the ER itself. Unlike somatic cells, little is known about the identity of the functionally distinct Ca²⁺ pool(s) in activating animal eggs.

How are these two functionally distinct Ca²⁺ pools involved during frog egg activation? It seems reasonable to hy-

pothesize that the production of Ins(1,4,5)P₃ by sperm-egg interaction triggers a local Ca²⁺ release from the Ins(1,4,5)-P₃-sensitive ER or cortical ER. This would result in a surface Ca²⁺ wave of Ins(1,4,5)P₃-induced Ca²⁺-release which in turn could stimulate Ca²⁺-induced Ca²⁺-release deeper in the egg where PIP₂ breakdown products might be less common. To test the above possibility it would be necessary to block the natural PIP₂ hydrolysis and determine if a normal Ca²⁺ wave could be induced by Ins(1,4,5)P₃ injection and subsequent Ca²⁺-induced Ca²⁺ release.

We are not sure whether the stratified eggs we studied were unactivated or activated. While the presence of CG along the entire stratified cortex suggests that the eggs were unactivated, we never observed an activation potential in these eggs despite injecting rather large levels of Ins(1,4,5)P₃ which would be expected to activate unactivated eggs. Ultrastructural examination of centrifuged eggs revealed no morphologically distinct cortical ER surrounding CG as found in uncentrifuged eggs. Therefore, it is possible that the normal Ca²⁺ release around the CGs could not occur in these stratified eggs.

References

1. Biden, T. J., C. B. Wollheim, and W. Schlegel. 1986. Inositol 1,4,5-trisphosphate and intracellular Ca²⁺ homeostasis in clonal pituitary cells (GH3): translocation of Ca²⁺ into mitochondria from a functionally discrete portion of the mitochondrial store. *J. Biol. Chem.* 261:7223–7229.
2. Busa, W. B. 1986. Measuring intracellular free calcium with single- and double-barreled ion-specific microelectrodes. *Prog. Clin. Biol. Res.* 210:57–70.
3. Busa, W. B., and R. Nuccitelli. 1985. An activated free cytosolic calcium wave follows fertilization in eggs of the frog, *Xenopus laevis. J. Cell Biol.* 100:1325–1329.
4. Busa, W. B., J. E. Ferguson, S. K. Joseph, J. R. Williamson, and R. Nuccitelli. 1985. Activation of frog (*Xenopus laevis*) eggs by inositol trisphosphate. I. Characterization of calcium release from intracellular stores. *J. Cell Biol.* 101:677–682.
5. Campanella, C., and P. Andreuccetti. 1977. Ultrastructural observations on cortical endoplasmic reticulum and on residual cortical granules in the egg of *Xenopus laevis. Dev. Biol.* 56:1–10.
6. Clapper, D. L., and H. C. Lee. 1985. Inositol trisphosphate induces calcium release from nonmitochondrial stores in sea urchin egg homogenates. *J. Biol. Chem.* 260:13947–13954.
7. Cuthertson, K. S. R., and P. H. Cobbold. 1985. Phorbol ester and sperm activate mouse oocytes by inducing sustained oscillations in cell calcium. *Nature (Lond.).* 316:541–542.
8. Cuthertson, K. S. R., D. G. Whittingham, and P. H. Cobbold. 1981. Free calcium increases in exponential phases during mouse oocyte activation. *Nature (Lond.).* 294:754–757.
9. Eberl, G., and K. Schnell. 1987. Ca²⁺ uptake and IP₃-induced Ca²⁺ release in permeabilized human lymphocytes. *FEBS (Fed. Eur. Biochem. Soc.) Lett.* 222:349–352.
10. Eisen, A., and G. T. Reynolds. 1984. Calcium transients during early development in single starfish (*Asterias forbesi*) oocytes. *J. Cell Biol.* 99:1878–1882.
11. Eisen, A., and G. T. Reynolds. 1985. Source and sinks for the calcium released during fertilization of single sea urchin eggs. *J. Cell Biol.* 100:1522–1527.
12. Eisen, A., D. P. Kiehart, S. W. Wieland, and G. T. Reynolds. 1984. Temporal sequence and spatial distribution of early events of fertilization in single sea urchin eggs. *J. Cell Biol.* 99:1647–1654.
13. Epel, D. 1980. Experimental analysis of the role of intracellular calcium in the activation of the sea urchin egg at fertilization. *In* The Cell Surface: Mediator of Developmental Processes. S. Subtelny and N. K. Wessels, editors. Academic Press, Inc., New York. 169–185.
14. Ferris, C. D., R. L. Huganir, S. Supattapone, and S. H. Snyder. 1989.

Purified inositol 1,4,5-trisphosphate receptor mediates calcium flux in reconstituted lipid vesicles. *Nature (Lond.)*. 342:87-89.

15. Furuichi, T., S. Yoshikawa, A. Miyawaki, K. Wada, N. Maeda, and K. Mikoshiba. 1989. Primary structure and functional expression of the inositol 1,4,5-trisphosphate-binding protein P$_{400}$. *Nature (Lond.)*. 342:32-38.

16. Gilkey, J. C., L. F. Jaffe, E. B. Ridgway, and G. T. Reynolds. 1978. A free calcium wave traverses the activating egg of the medaka, *Oryzias latipes*. *J. Cell Biol.* 76:448-466.

17. Hafner, M., C. Petzelt, R. Nobiling, J. B. Pawley, D. Kramp, and G. Schatten. 1988. Wave of free calcium at fertilization in the sea urchin egg visualized with fura-2. *Cell Motil. Cytoskeleton*. 9:271-277.

18. Hashimoto, S., B. Bruno, D. P. Lew, T. Pozzan, P. Volpe, and J. Meldolesi. 1988. Immunocytochemistry of calciosomes in liver and pancreas. *J. Cell Biol.* 107:2523-2531.

19. Ilundain, A., J. A. O'Brien, K. A. Burton, and F. V. Sepulveda. 1987. Inositol trisphosphate and calcium mobilisation in permeabilized enterocytes. *Biochim. Biophys. Acta*. 896:113-116.

20. Iwamatsu, T., Y. Hoshimoto, and Y. Hiramoto. 1988. Mechanism of Ca^{2+} release in medaka eggs microinjected with inositol 1,4,5-trisphosphate and Ca^{2+}. *Dev. Biol.* 129:191-197.

21. Jaffe, L. F. 1980. Calcium explosions as triggers of development. *Ann. NY Acad. Sci.* 339:86-101.

22. Jean, T., and C. B. Klee. 1986. Calcium modulation of inositol 1,4,5-trisphosphate-induced calcium release from neuroblastoma x glioma hybrid (NG 108-15) microsomes. *J. Biol. Chem.* 261:16414-16420.

23. Jy, W., and D. H. Haynes. 1988. Calcium uptake and release characteristics of the dense tubules of digitonin-permeabilized human platelets. *Biochim. Biophys. Acta*. 944:374-382.

24. Kline, D., L. Simoncini, G. Mandel, R. A. Maue, R. T. Kado, and L. A. Jaffe. 1988. Fertilization events induced by neurotransmitters after injection of mRNA in *Xenopus* eggs. *Science (Wash. DC)*. 241:464-467.

25. Kubota, H. Y., Y. Yoshimoto, M. Yoneda, and Y. Hiramoto. 1987. Free calcium wave upon activation in *Xenopus* eggs. *Dev. Biol.* 119:129-136.

26. Luby-Phelps, K., F. Lanni, and D. L. Taylor. 1988. The submicroscopic properties of cytoplasm as a determinant of cellular function. *Ann. Rev. Biophys. Biophys. Chem.* 17:369-396.

27. Masui, Y. 1972. Distribution of the cytoplasmic activity inducing germinal vesicle breakdown in frog oocytes. *J. Exp. Zool.* 179:365-378.

28. Miyazaki, S. 1988. Inositol 1,4,5-trisphosphate-induced calcium release and guanine nucleotide-binding protein-mediated periodic calcium rises in golden hamster eggs. *J. Cell Biol.* 106:345-353.

29. Miyazaki, S., N. Hashimoto, Y. Yoshimoto, T. Kishimoto, Y. Igusa, and Y. Hiramoto. 1986. Temporal and spatial dynamics of the periodic increase in intracellular free calcium at fertilization of golden hamster eggs. *Dev. Biol.* 118:259-267.

30. Muldoon, L. L., G. A. Jamieson, Jr., and M. L. Villereal. 1987. Calcium mobilization in permeabilized fibroblasts: effects of inositol trisphosphate, orthovanadate, mitogens, phorbol ester, and guanosine triphosphate. *J. Cell. Physiol.* 130:29-36.

31. Mullaney, J. M., M. Yu, T. K. Ghosh, and D. L. Gill. 1988. Calcium entry into the inositol 1,4,5-trisphosphate-releasable calcium pool is mediated by a GTP-regulatory mechanism. *Proc. Natl. Acad. Sci. USA*. 85:2499-2530.

32. Munoz, J.-L., F. Deyhimi, and J. A. Coles. 1983. Silanization of glass in the making of ion-sensitive microelectrodes. *J. Neurosci. Methods*. 8:231-247.

33. Nakamura, Y., and S. Ohtaki. 1987. Calcium release from porcine thyroid microsomes by phosphatidylinositol 4,5-bisphosphate and inositol 1,4,5-trisphosphate. *Endocrinology*. 120:2302-2307.

34. Nuccitelli, R., D. J. Webb, S. T. Lagier, and G. B. Matson. 1981. ^{31}P NMR reveals increased intracellular pH after fertilization in *Xenopus* eggs. *Proc. Natl. Acad. Sci. USA*. 78:4421-4425.

35. Nuccitelli, R., D. Kline, W. B. Busa, R. Talevi, and C. Campanella. 1988. A highly localized activation current yet widespread intracellular calcium increase in the egg of the frog, *Discoglossus pictus*. *Dev. Biol.* 130:120-132.

36. Payne, R., and A. Fein. 1987. Inositol 1,4,5 trisphosphate releases calcium from specialized sites within *Limulus* photoreceptors. *J. Cell Biol.* 104:933-937.

37. Purves, R. D. 1981. Microelectrode Methods for Intracellular Recording and Iontophoresis. Academic Press, Inc., London. 92.

38. Rengasamy, A., and H. Feinberg. 1988. Inositol 1,4,5-trisphosphate-induced calcium release from platelet plasma membrane vesicles. *Biochem. Biophys. Res. Commun.* 150:1021-1026.

39. Ridgway, E. B., J. C. Gilkey, and L. F. Jaffe. 1977. Free calcium increases explosively in activating medaka eggs. *Proc. Natl. Acad. Sci. USA*. 74:623-627.

40. Ross, C. A., J. Meldolesi, T. A. Milner, T. Satoh, S. Supattapone, and S. H. Snyder. 1989. Inositol 1,4,5-trisphosphate receptor localized to endoplasmic reticulum in cerebellar Purkinje neurons. *Nature (Lond.)*. 339:468-470.

41. Rossier, M. F., K.-H. Krause, P. D. Lew, A. M. Capponi, and M. B. Vallotton. 1987. Control of cytosolic free calcium by intracellular organelles in bovine adrenal glomerulosa cells. *J. Biol. Chem.* 262:4053-4058.

42. Shah, J., R. S. Cohen, and H. C. Pant. 1987. Inositol trisphosphate-induced calcium release in brain microsomes. *Brain Res.* 419:1-6.

43. Shen, S. S., and L. J. Burgart. 1986. 1,2-diacylglycerols mimic phorbol 12-myristate 13-acetate activation of the sea urchin egg. *J. Cell. Physiol.* 127:330-340.

44. Snyder, S. H., and S. Supattapone. 1989. Isolation and functional characterization of an inositol trisphosphate receptor from brain. *Cell Calcium*. 10:337-342.

45. Spitzer, J. A., and I. V. Deaciuc. 1987. IP$_3$-dependent Ca^{2+} release in permeabilized hepatocytes of endotoxemic and septic rats. *Am. J. Physiol.* 253:E130-134.

46. Steinhardt, R., R. Zucker, and G. Schatten. 1977. Intracellular calcium release at fertilization in the sea urchin egg. *Dev. Biol.* 58:185-196.

47. Swann, K., and M. Whitaker. 1985. Stimulation of the Na/H exchanger of sea urchin eggs by phorbol ester. *Nature (Lond.)*. 314:274-277.

48. Swann, K., and M. Whitaker. 1986. The part played by inositol trisphosphate and calcium in the propagation of the fertilization wave in sea urchin eggs. *J. Cell Biol.* 103:2333-2342.

49. Taylor, C. W., and J. W. Putney, Jr. 1985. Size of the inositol 1,4,5-trisphosphate-sensitive calcium pool in guinea-pig hepatocytes. *Biochem. J.* 232:435-438.

50. Thomas, M. V. 1982. Techniques in Calcium Research. Academic Press, Inc., New York. 214 pp.

51. Tsien, R. Y., and M. Poenie. 1986. Fluorescence ratio imaging: a new window into intracellular ionic signaling. *Trends Biochem. Sci.* 11:450-459.

52. Tsien, R. Y., and T. J. Rink. 1980. Neutral-carrier ion-selective microelectrodes for measurement of intracellular free calcium. *Biochim. Biophys. Acta*. 599:623-638.

53. Tsien, R. Y., and T. J. Rink. 1981. Calcium-selective electrodes: a novel PVC-gelled neutral carrier mixture compared with other currently available sensors. *J. Neurosci. Methods*. 4:73-89.

54. Turner, P. R., L. A. Jaffe, and A. Fein. 1986. Regulation of cortical vesicle exocytosis in sea urchin eggs by inositol 1,4,5-trisphosphate and GTP-binding protein. *J. Cell Biol.* 102:70-76.

55. Turner, P. R., L. A. Jaffe, and P. Primakoff. 1987. A cholera toxin-sensitive G-protein stimulates exocytosis in sea urchin eggs. *Dev. Biol.* 120:577-583.

56. Ueda, T., S.-H. Chueh, M. K. Noel, and D. L. Gill. 1986. Influence of inositol 1,4,5-trisphosphate and guanine nucleotides on intracellular calcium release within the N1E-115 neuronal cell line. *J. Biol. Chem.* 261:3184-3192.

57. Volpe, P., K. H. Krause, S. Hashimoto, F. Zorzato, T. Pozzan, J. Meldolesi, and D. P. Lew. 1988. Calciosome, a cytoplasmic organelle: the inositol 1,4,5-trisphosphate-sensitive Ca^{2+} store of non-muscle cells? *Proc. Natl. Acad. Sci. USA*. 85:1091-1095.

58. Webb, D. J., and R. Nuccitelli. 1982. Intracellular pH changes accompany the activation of development in frog eggs: comparison of pH microelectrode and ^{31}P-NMR measurements. *In* Intracellular pH, its Measurement, Regulation, and Utilization in Cellular Functions. R. Nuccitelli and D. W. Deamer, editors. Alan R. Liss, Inc., New York. 293-324.

59. Whitaker, M., K. Swann, and I. Crossley. 1989. What happens during the latent period at fertilization. *In* Mechanisms of Egg Activation. R. Nuccitelli, G. N. Cherr, and W. H. Clark, editors. Plenum Publishing Corp., New York. 157-171.

60. Winkler, M. M., R. A. Steinhardt, J. L. Grainger, and L. Minning. 1980. Dual ionic control for the activation of protein synthesis at fertilization. *Nature (Lond.)*. 287:558-560.

61. Yoshii, N., M. Mio, and K. Tasaka. 1988. Ca uptake and Ca releasing properties of the endoplasmic reticulum in rat peritoneal mast cells. *Immunopharmacology*. 16:107-113.

62. Yoshimoto, Y., T. Iwamatsu, K. Hirano, and Y. Hiramoto. 1986. The wave pattern of free calcium release upon fertilization in medaka and sand dollar eggs. *Dev. Growth. & Differ.* 28:583-596.

1110